



Review

Optofluidic Tunable Lenses for In-Plane Light Manipulation

Qingming Chen ¹, Tenghao Li ¹, Zhaohui Li ², Jinlin Long ³ and Xuming Zhang ^{1,4,*}

¹ Department of Applied Physics, The Hong Kong Polytechnic University, Hong Kong 999077, China; qing-ming.chen@connect.polyu.hk (Q.C.); 14900295r@connect.polyu.hk (T.L.)

² School of Electronics and Information Technology, Sun Yat-Sen University, Guangzhou 510275, China; li_zhaohui@hotmail.com

³ School of Chemistry and Chemical Engineering, Fuzhou University, Fuzhou 350116, China; jllong@fzu.edu.cn

⁴ Shenzhen Research Institute of the Hong Kong Polytechnic University, Shenzhen 518057, China

* Correspondence: apzhang@polyu.edu.hk; Tel.: +852-3400-3258

Received: 22 January 2018; Accepted: 11 February 2018; Published: 26 February 2018

Abstract: Optofluidics incorporates optics and microfluidics together to construct novel devices for microsystems, providing flexible reconfigurability and high compatibility. Among many novel devices, a prominent one is the in-plane optofluidic lens. It manipulates the light in the plane of the substrate, upon which the liquid sample is held. Benefiting from the compatibility, the in-plane optofluidic lenses can be incorporated into a single chip without complicated manual alignment and promises high integration density. In term of the tunability, the in-plane liquid lenses can be either tuned by adjusting the fluidic interface using numerous microfluidic techniques, or by modulating the refractive index of the liquid using temperature, electric field and concentration. In this paper, the in-plane liquid lenses will be reviewed in the aspects of operation mechanisms and recent development. In addition, their applications in lab-on-a-chip systems are also discussed.

Keywords: optofluidics; microfluidics; in-plane liquid lens; lab-on-a-chip

1. Introduction

Nowadays, miniaturized systems are playing important roles in both academic research and industrial applications. More elements and functions have been incorporated into a single chip, reducing the cost and improving the performance at the same time. Optofluidics combines optics and microfluidics together to construct novel elements for lab-on-a-chip applications [1–7]. By replacing the solid materials with liquids, it enables the flexible modulation of optical properties and improves compatibilities. Compared with its solid counterpart, optofluidics has some unique merits [8–11], such as flexible tunability, good compatibility, small size and easy fabrication, etc. It has been intensively studied by numerous research communities [1–3,7,12,13]. A number of applications have been achieved using the optofluidic techniques, such as chemical and biological detection [4,5,14], particle manipulation [15,16], optofluidic laser [13,17], tunable waveguides [18,19], and reconfigurable optofluidic lens [12]. Among them, the optofluidic lens is the most extensive exploited part. In conventional optical systems, the optical lens is used to change the propagation of light and reshape the beam. The solid lens has constant refractive index (RI) and a fixed focal length. The optical modulation is achieved by mechanical movement, which is complicated and poorly scalable. While the optofluidic lens enables easy modulation of the optical properties by either changing the lens geometry or tuning RI of the liquid.

By the manipulation of liquids in microscale, reconfigurable optofluidic lens has been demonstrated in a small chip. According to the propagation of the beam, the liquid lenses can

be generally classified into two categories: out-of-plane lens and in-plane lens [12]. The former manipulates the beam in the direction perpendicular to the substrate of microfluidic chip [20], which is similar to the conventional lens. It can be used to replace the solid lens in some miniature optical systems that require variable focusing. The latter deals with the light in the direction parallel to the substrate of microfluidic chip, providing an effective way to manipulate the beam in a microfluidic network. Therefore, the sample and the probe beam can be delivered in the same liquid layer, enhancing the interaction of light and matter. Thus, it promises better scalability and more complexity for optofluidic networks. Some reviews have reported the development and applications of the optofluidic lenses [12,21–23]. Nam-Trung Nguyen gave a comprehensive review of the optofluidic lenses on their categories and working principles [12]. It focused on the schematic designs of different optofluidic lenses and some characteristic parameters, such as the response time and the tunability of focal length and RI. It also listed some liquids that are widely used in optofluidics. Mishra et al. reported the general characteristics and characterization methods of the optofluidic lenses, including the actuation methods and the spherical aberration [22]. In particular, Mishra had deeply discussed the aberration control, which is very important in optical imaging. Xu et al. discussed the development of dielectrophoretically tunable optofluidic lenses [23]. And Krogmann presented the design, fabrication and optical properties of the electrowetting based micro-optical components [24]. However, a comprehensive description of in-plane liquid lenses and their perspectives in optofluidic networks is still required. This review focuses on the in-plane optofluidic lenses, including the working mechanisms and their applications in lab-on-a-chip systems.

Figure 1a summarizes the categories of the in-plane lenses and Figure 1b explains the corresponding working principles. Most of the reported designs of in-plane optofluidic lenses can be classified into two types: refractive lens and gradient index (GRIN) lens. The former often makes use of interfacial deformation and the latter of RI modulation. The rest of reported designs can be generally grouped into the others in this review. In the refractive lens, the beam is refracted at the smooth fluidic interface of immiscible liquids (see Figure 1(b1)). The focal length is usually tuned by changing the lens geometry. In a microfluidic chip, there are numerous ways to modify the curvature of the fluidic interface, for example, pressure control [25], hydrodynamic modulation [26,27], electrowetting [24] and dielectrophoresis [23]. Among them, the pressure control and the hydrodynamic modulation are more popular in regulating in-plane lenses. In the GRIN lens, solution diffusion [28] or thermal diffusion [29,30] can be used to establish a RI gradient profile, in which the rays are bent gradually and then focused to a point (Figure 1(b2)). A large RI gradient (usually over 0.1) is achievable in a microscale region, resulting in tight focusing and wide tunable range. The refractive lens and the GRIN lens are often independent of the polarization and the wavelength of the incident light due to the use of isotropic and low-dispersion liquids (e.g., water, ethanol, ethylene glycol). In addition, there are some other lenses that aim at polarization separation or wavelength selection, such as birefringent liquid lens [31] and diffractive optofluidic lens [32]. For example, liquid crystal (LC) has been used to construct a polarization-dependent liquid lens [31]. Figure 1(b3) displays the schematic of the LC liquid lens, in which the LC molecules can be realigned by applying a sufficiently strong electrical field. As a result, incident beams of different polarization directions would experience different RIs and have different focal lengths. Another kind of lens is Fresnel zone plate (FZP), which is based on the diffraction rather than refraction. As shown in Figure 1(b4), an optofluidic FZP can be achieved for light manipulation by filling liquid into the periodic microstructure. Different parts of the diffracted lights interference constructively with each other to form a focal point. The FZP depends on the incident wavelength, providing another freedom of tunability.

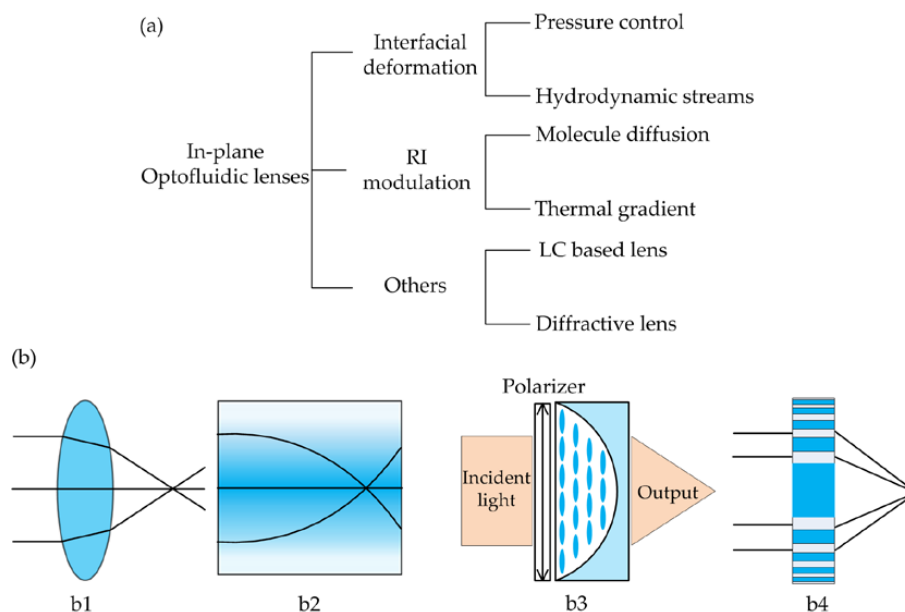


Figure 1. In-plane optofluidic lenses categories and the working principles: (a) The in-plane liquid lenses are classified into three types of lenses according to their working principles; (b) schematic diagrams of the in-plane liquid lens: (b1) is the interfacial deformation lens; (b2) is RI modulation (gradient index) lens; (b3) is the liquid-crystal based lens (LC: the blue ellipses) and (b4) is the diffractive lens (i.e., the Fresnel zone plate).

This article has five sections. The first gives an introduction of optofluidic lenses. In the second, the in-plane optofluidic lenses will be discussed according to their operation mechanisms. Then, some applications of the in-plane liquid lenses will be presented in the third section. There is a brief discussion in section four. The last part is the conclusion.

2. Classification of In-Plane Optofluidic Lenses

In this part, the in-plane optofluidic lenses will be reported based on their operation mechanisms. Firstly, some example of the refractive lenses based on the fluidic interfaces will be presented. Then the GRIN lenses are discussed. In addition, the in-plane liquid lenses based on other methods are also discussed at the end of this section.

2.1. Interfacial Deformation

The most straightforward method to construct an in-plane optofluidic tunable lens is to use the interfaces between immiscible streams (or liquid-air interface), where the interfacial curvature can be modified by numerous microfluidic techniques [25,26,33]. The general working principle is depicted in Figure 1(b1). In the case of in-plane lens, the geometry modulation can be achieved either by the pressure control or by the hydrodynamic streams. In the pressure-control liquid lens, the curvature of the liquid-air interface is modified by external pumping [25,34]. Tony Huang's group proposed a reconfigurable in-plane liquid lens using fluidic pressure to tune the liquid/air interface in a microfluidic chip [25]. As shown in Figure 2a, this microlens consists of a reconfigurable divergent liquid-air interface and a static polydimethylsiloxane (PDMS) lens. The liquid flows through a straight channel and traps the air in the chamber, forming a liquid-air interface. By adjusting the flow rate, it changes the pressure inside the channel as well as the interfacial radius. It demonstrated the continuous modulation of the focal length by tuning the flow velocity. Behind the lens, there is a chamber for experimental raytracing. Another pressure-controllable liquid-air in-plane lens is demonstrated by Dong et al. [34]. By precisely locating a liquid droplet at the T-shape junction, a tunable in-plane liquid lens is formed in the microchannel (see Figure 2b). This microlens has

a tunable focal length from a few hundreds of micrometers to infinite. It can be pneumatically repositioned and removed inside the predefined microchannel. The geometry of the chamber can also be used as a tunable lens by modifying the shape using the pressure control [35]. The pressure-control liquid-air interface is governed by the Laplace law:

$$\Delta P = 2\gamma\kappa = \gamma\left(\frac{1}{R_1} + \frac{1}{R_2}\right) \quad (1)$$

where γ is the surface tension coefficient between the liquid and air, κ is the mean curvature of the liquid-air interface. R_1 (in horizontal) and R_2 (in vertical) are the principal curvature radii of the interface. The ideal liquid-air interface is spherical in both horizontal and vertical directions. The external pump is used to balance at the pressure drop at the interface [25,34].

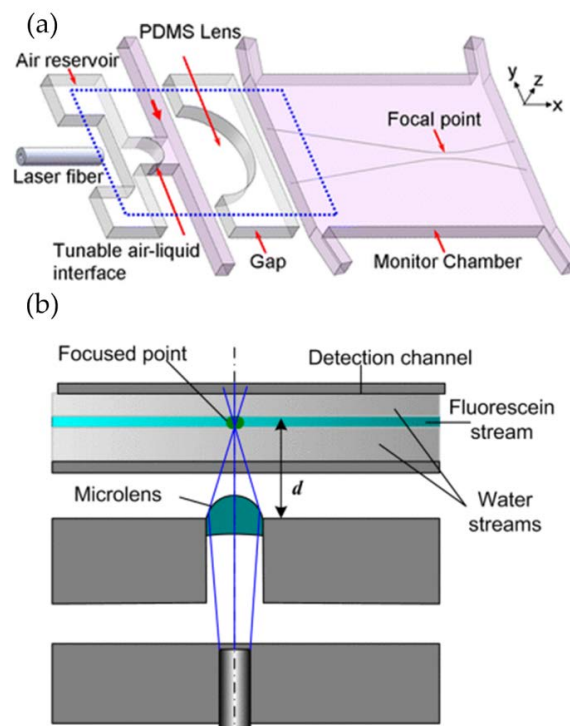


Figure 2. Pressure-control liquid lenses: (a) liquid-air interface tuned by flow rate control [25]; (b) pneumatically droplet tunable lens [34].

Another way to change the geometry of the in-plane liquid lens is to use the hydrodynamic modulation [26,27,33], in which the fluidic curve is formed and controlled by hydrodynamic force. In this case, two or more immiscible streams (the liquid core and the liquid cladding) are pumped into a specific microchannel to form reconfigurable interfaces. Tuning the ratio of the flow streams enables to continuously modulate the fluidic interfaces. It should be noted that the optical properties of the hydrodynamic stream liquid lens are dependent on the shape of the fluidic chamber. Seow et al. demonstrated a tunable liquid lens by injecting three flow streams into a rectangle-shaped expansion chamber [36], where the liquid with a higher RI acts as the core and the other two streams with a lower RI act as the cladding. Figure 3 shows the schematic designs of the liquid lenses, V_{co} is the flow rate of the core, V_{cll} and V_{clr} are the flow rates of the left and right claddings, respectively. A biconvex lens is formed when $V_{co} > V_{clr} = V_{cll}$, see Figure 3a. And the curvature radius becomes smaller with a higher cladding flow rate. By increasing the value of V_{clr} , the microlens becomes plano-convex (Figure 3b) and then concave-convex (Figure 3c), respectively. Both collimation and focusing have been demonstrated in this type of microlens by tuning the flow rates.

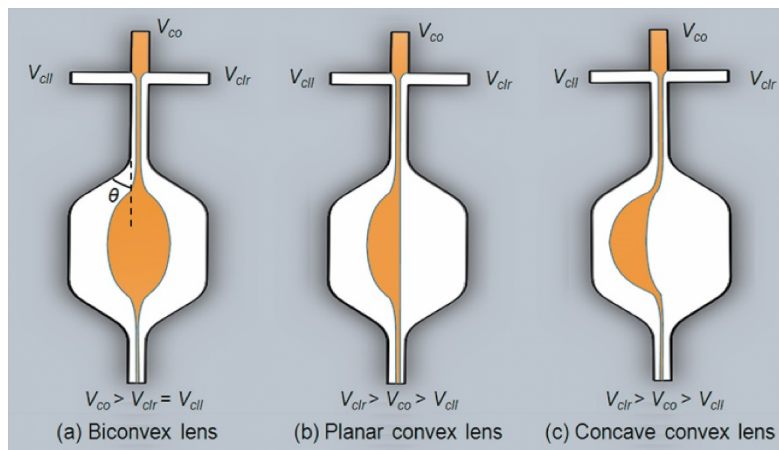


Figure 3. Different curvatures of tunable liquid microlenses via the control of laminar flow rate [36]: (a) biconvex lens; (b) plano-convex lens; (c) concave-convex lens.

Another design of liquid lens uses the circular chamber as shown in Figure 4. Song et al. reported the modeling and experimental results of a tunable lens by injecting three laminar streams into a circular chamber [37]. The liquid-core liquid-cladding lens with perfect curvatures was formed by the circular design. Figure 4 describes the schematic design of the circular liquid lens. In the symmetric state, the lens has a biconvex shape as shown in Figure 4a. By further increasing the flow rate of inlet C, it can tune the lens into the plano-convex shape (Figure 4b) and then the concave-convex shape (Figure 4c). The curvature radius can be tuned from that of the chamber to infinity. As the width of the channel is much smaller than that of the expansion chamber, the model can be approximately described as a source-sink pair model [37]. A reconfigurable biconcave lens was demonstrated by Li et al. [38]. They used the combination of pressure driven flow and electro-osmosis to realize both focusing and diverging in a rectangle chip. Fang et al. proposed a hydrodynamically reconfigurable optofluidic lens, which can be tuned from biconcave to biconvex [27]. Figure 5 depicts the operation principle of the liquid lens. The chamber with two convex ends is used to realize the modulation from biconcave to biconvex. Two immiscible liquids with different RIs are injected into the expansion chamber, where the liquid core (with higher RI) is sandwiched by the liquid claddings (with lower RI). The curvature of the interface is modified by tuning the flow ratio of the core and cladding streams. When the cladding flow is low, the liquid core expands outside into the cladding area, resulting in a biconvex lens (see Figure 5a,b). By increasing the rate of the cladding flow, the curvature of the liquid lens decreases. With the further increase of the cladding flow, the liquid core is compressed into a biconcave shape and the lens becomes negative, as shown in Figure 5c,d. The modulation from biconvex (positive) to biconcave (negative) lens has been demonstrated by adjusting the flow rate. They proposed a two-dimensional quadrupolar flow model to analyze the operation of the liquid lens [27]. As shown in Figure 6, the model has two sources at the left side and two sinks at the right side. The sources and sinks were regarded as dimensionless points. By combining the flow model and the theory of thick lens together, an equation was derived to describe the focal length:

$$f = \frac{-n_1 r^2}{2(n_1 - n_0)[(n_1 - n_0)(s + b) - n_1 r]} \quad (2)$$

where n_0 and n_1 are the RIs of the liquid cladding and liquid core, respectively. And b is half of the distance between the two sources, r is the curvature radius of the liquid interface. The parameter s equals to d or $-d$ when the interface is positive or negative, respectively. By using the combination of a tunable biconvex lens and a reconfigurable liquid prism. Chao et al. demonstrated the controlling of the focal length and the deviation angle of the beam [39].

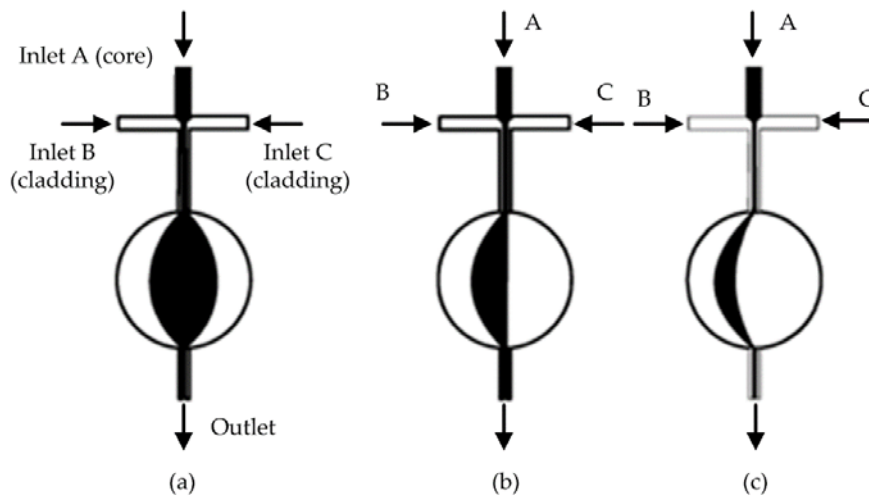


Figure 4. Reconfigurable optofluidic lenses with a circular lens chamber [37]: the lens shape is modified by adjusting the flow rates of the core and cladding streams. (a) biconvex lens; (b) plano-convex lens; (c) concave-convex lens.

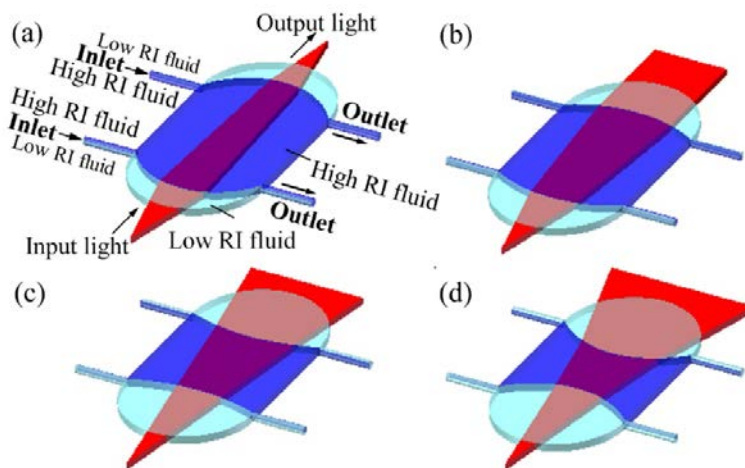


Figure 5. Hydrodynamically reconfigurable optofluidic lens, in which the liquid core (in blue) is sandwiched by the liquid claddings [27]. (a) The liquids form a biconvex lens and the beam is focused. (b) The beam is collimated when the interface curvature becomes smaller. (c,d) A biconcave lens is obtained and the beam becomes divergent.

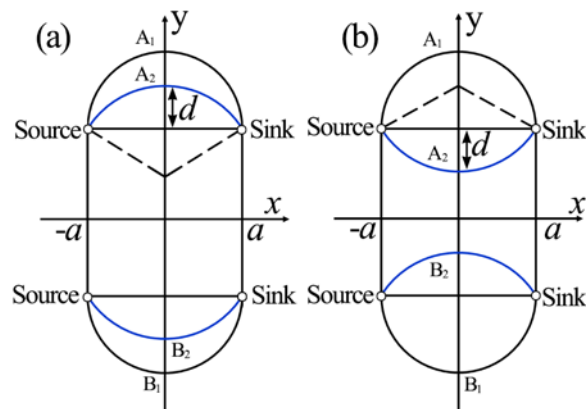


Figure 6. The coordinate of microlens model [27].

2.2. Refractive Index (RI) Modulation

As mentioned above, the RI modulation is another way to alter the optical properties of fluidic components. A simple method to change the RI of the liquid medium is to replace one with another. Seow et al. proposed a tunable planar optofluidic lens using a PDMS lens chamber [40]. By filling the chamber with the mixer of two miscible liquids, the RI was tuned from 1.33 to 1.63. The RI of medium is dependent on several physical properties such as concentration [28,41] and temperature [30]. It can be also changed by external electric field, acoustic field and mechanical strain. The optical properties of the optofluidic device can be tuned through the modulation of the RI profile, which is also very popular in solid optics. For instance, in a graded index optical fiber, rays follow sinusoidal paths and cross each other periodically. Similarly, rays bend gradually and focus to a focal point, forming the GRIN lens. Compared with the solid materials, the RI modulation of liquid is much easier. By simply changing the concentration of the solutions, the RI change over 0.1 can be achieved [21]. A variety of optofluidic waveguides [19,42,43] and lenses [28,44] based on the diffusion of two miscible solutions have been demonstrated. Temperature gradient is another effective way to form a RI gradient in fluid [30].

A simple method to form a RI gradient within liquid medium is solute diffusion. In a laminar flow inside the microchannel, the concentration gradient is determined by the solution diffusion [45], which can be modulated by the flow rate control. Therefore, a graded RI profile can be achieved using the solution diffusion. Yang et al. proposed an optofluidic RI gradient for lightwave bending and manipulation through the diffusion between ethylene glycol and deionized water [19], in which the RI can be tuned from 1.34 to 1.42. Mao et al. demonstrated a reconfigurable liquid gradient index (L-GRIN) lens with two degrees of freedom using CaCl₂ solution as the core and deionized water as the cladding [28]. As shown in Figure 7A, the two liquids (the CaCl₂ solution and DI water) are injected into the microfluidic chip to establish the gradient profile by diffusion of laminar flows. The rays bend gradually when they meet the RI gradient. Tuning the flow rates of the liquids enables not only to change the focal length, but also to shift the focused beam away from the optical axis, providing another freedom for adaptive optics. Figure 7B depicts the RI distribution along lines 1–5. The RI profile inside the channel follows a hyperbolic secant (HS) function as

$$n^2(x) = n_s^2 + (n_0^2 - n_s^2) \operatorname{sech}^2(\alpha x) \quad (3)$$

where $n(x)$ is the RI at the given position, n_0 is the RI at the center, n_s is the lowest RI in the liquid medium and α is the gradient parameter. Changing the flow rate enables the modulation of the RI profile as well as the focal length of the lens. Figure 7C shows the RI along line 3 at different flow rates. The ray tracing simulated results in different flow conditions are shown in Figure 7D. It can also shift the focus away from the center using an asymmetric RI profile.

Zhao et al. further improved the performance of the diffusion based optofluidic lens by upgrading the lens design [44], see Figure 8a. By adding a fluidic mixer before the lens section, a HS RI profile can be achieved by precisely controlling the flow rates of the mixer. Borrowed the idea from aberration-free Maxwell's fisheye lens, such a structure is demonstrated to have a lower spherical aberration (see Figure 8b). It is able to focus the beams to different shifted positions on the same focal plane (Figure 8c).

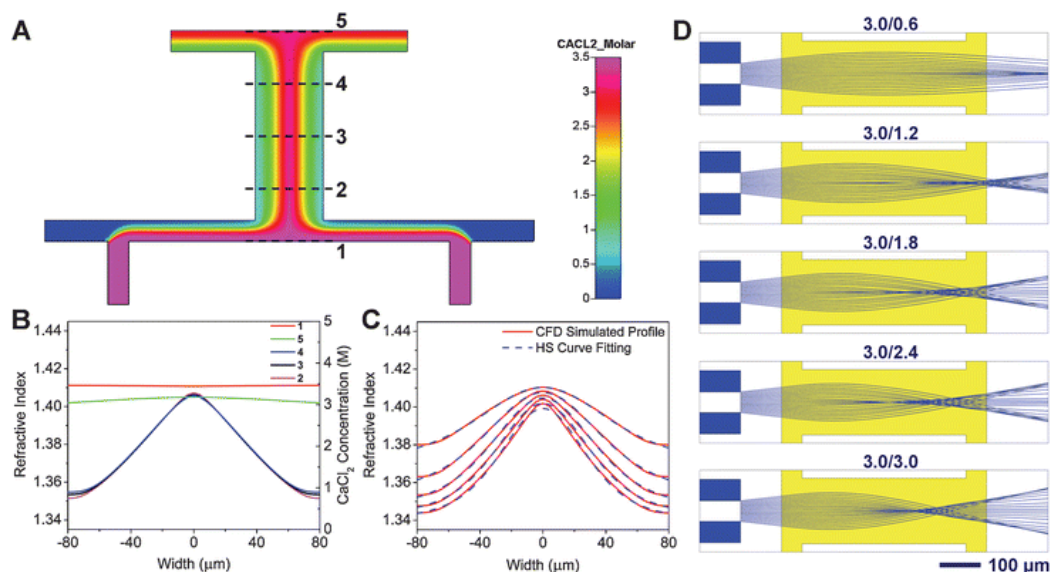


Figure 7. L-GRTN lens with two degrees of freedom [28]. (A) Simulated refractive index profile and ray tracing. (B) Cross-sectional refractive index distribution at different locations along the flow direction (1, 2, 3, 4 and 5 as indicated in a). (C) Refractive index distribution along line 3 (defined in a) at different flow rates. (D) Ray tracing results in different flow conditions (3.0/0.6 represents CaCl₂ flow rates = 3.0 μL m⁻¹ and H₂O flow rate = 0.6 μL m⁻¹, respectively).

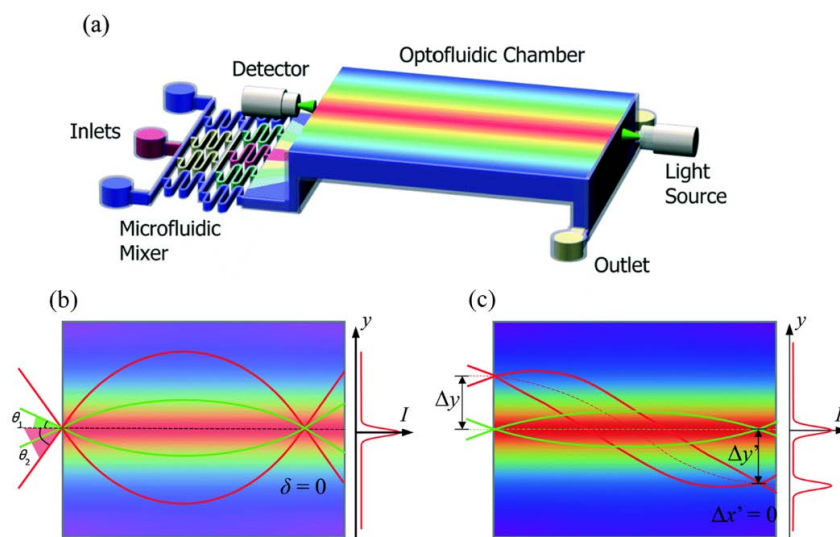


Figure 8. Schematic and working principle of the optofluidic lens [44]. (a) Design of the optofluidic chip; (b) Spherical aberration; (c) Field curvature aberration.

Temperature conduction is another effective way to form a graded RI profile for beam manipulation in microfluidics. According to the thermal lens effect, the RI decreases linearly while the temperature is increased. Therefore, the RI is lower at the hot region. The rays gradually bend while experiencing an inhomogeneous temperature field. As the magnitude of the thermal conduction coefficient is about two orders larger than that of the molecular diffusion coefficient, the thermal lens effect promises a faster response speed. But the thermos-optics coefficient is relative small, which has a value of $1\sim 10 \times 10^{-4} \text{ K}^{-1}$. For instance, water has a thermo-optics coefficient of $-1.2 \times 10^{-4} \text{ K}^{-1}$ at $0\sim 80 \text{ }^\circ\text{C}$. The thermal-induced RI is at the order of 0.01, which is much smaller as compared to that derived from the concentration gradient. Tang et al. proposed a thermal-induced

optical waveguide by the streams at different temperatures [18]. It utilized two streams at higher temperature (the cladding) to sandwich another stream at lower temperature (the core) to form a temperature gradient across the channel. By simply changing the flow rate, the optical properties of the liquid waveguide can be modified. In our previous work, we presented an optofluidic tunable lens using the laser-induced thermal gradient, in which a RI gradient is established in microscale for focusing. As shown in Figure 9, a pump laser is utilized to illuminate the two metal patterns (the yellow pads in Figure 9a), which absorb the light and heat up the flowing liquid (benzyl alcohol, $dn/dT = 4 \times 10^{-4} \text{ K}^{-1}$). A temperature induced RI gradient is established inside the microchannel for beam manipulation. Different from the conventional GRIN lenses, this laser-induced thermal lens has a 2D RI gradient, in which the cross-sectional RI follows the square-low parabolic function as described by

$$n(r,z) = n_{c,z} \sqrt{1 - A_z r^2} \quad (4)$$

where $n(r,z)$ is the RI at point (r,z) and z is the coordinate position along the flow direction. $n_{c,z}$ is the RI at the central position ($r = 0,z$), and A_z is the parabolic parameter. The simulated 3D- and 2D-RI profiles are shown in Figure 9b,c, respectively. The rays bend gradually and focus to a point while passing the gradient section in between the two metal strips (see Figure 9a). This optofluidic lens allows to use only one liquid. The pump laser enables noncontact modulation and free relocation of the lens region.

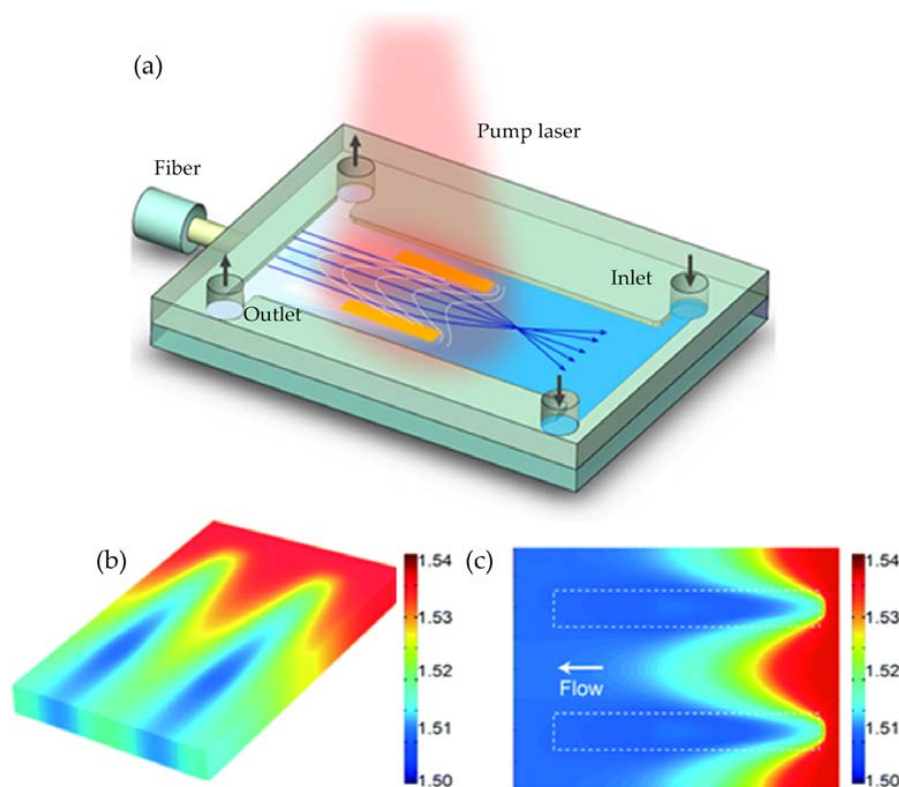


Figure 9. Optofluidic thermal lens using laser-induced thermal gradient [29]: (a) schematic design; (b) 3D and (c) 2D RI profiles.

2.3. Others

Apart from the above mentioned liquid lenses, there are other types of in-plane optofluidic lenses that can also be used for beam manipulation in microfluidic networks.

In the conventional hydrodynamic liquid-liquid lens, isotropic liquids are used as the core and the cladding, which are polarization independent. However, a polarization-dependent device may

find special applications in which the polarized light is preferred. A commonly used polarizable liquid is the LC that has a state between isotropic liquid and totally anisotropic solid crystal, resulting in a partially anisotropic fluid. One of the LC phases is nematic, which is usually uniaxial. It has a preferred long axis and a short axis. The nematic LCs have the fluidic properties similar to ordinary organic liquids, but they can be well aligned by a sufficiently strong electric field. Therefore, the nematic LCs have been widely used in electrically reconfigurable optical devices, such as liquid crystal display. Numerous LC lenses have also been demonstrated [46]. The incident light experiences different RIs according to its polarization. The effective RI can be expressed by

$$n_{eff} = n_o n_e \sqrt{\frac{1}{n_o^2 \cos^2 \theta + n_e^2 \sin^2 \theta}} \tag{5}$$

where θ is the angle between the LC rod and the polarization of the incident light, n_e and n_o are the extraordinary RI and the ordinary RI of the LC molecule, respectively. It is noted that n_{eff} varies from n_o to n_e according to the wave polarization.

Wee et al. demonstrated an in-plane optofluidic birefringent lens by manipulating the streams of a nematic LC and an isotropic liquid under an external electric field [31]. Figure 10 shows the schematic design, in which the nematic LC and the isotropic liquid are used for the main stream and the surrounding sub-streams, respectively. When an external electric field is applied in the direction perpendicular to the substrate, the LC molecules are reoriented along the electric field, resulting in the birefringent effect in the liquid layer. As n_e and n_o have different values in the nematic LC, the RI difference (i.e., the RI contrast on two sides of the interface) is dependent on the polarization state of the incident light. For the p-polarized light, the effective index equals to n_o , which is smaller than n_e . Therefore, the RI contrast ($\Delta n = n_{eff} - n_i$) of the p-mode is smaller than that of the s-mode. As a consequence, the s-mode has a smaller focal length (see Figure 10b) than that of the p-mode (Figure 10a). This new type of hydrodynamic optofluidic lens can be modulated by either the flow rate or the polarization of the incident light.

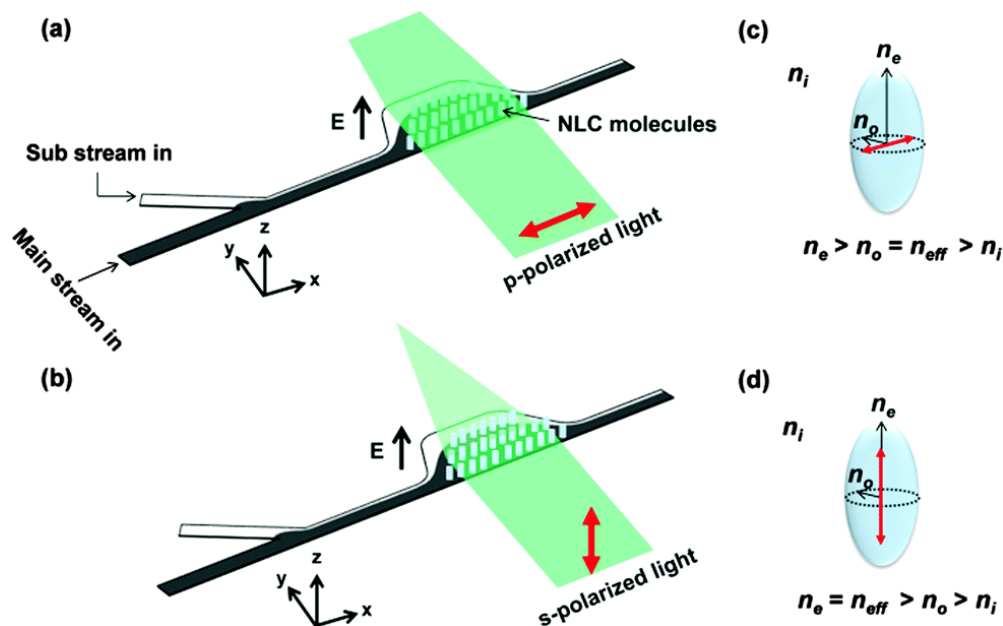


Figure 10. Schematic of the birefringent optofluidic lens [31]: the focusing effect of (a) p-polarized and (b) s-polarized light. Index ellipsoids are used to describe the RI of (c) p-polarized and (d) s-polarized light. The red arrows indicate the direction of polarization.

The traditional lenses focus the light due to the reflection or refraction. While in a Fresnel zone plate (FZP), the light is focused by diffraction, which is wavelength dependent. Inspired by this idea, Yang's group demonstrated an optofluidic FZP used a solid-liquid hybrid structure [32] (see Figure 11). It utilizes a microfluidic mixer to prepare the liquid with a specific RI, which is delivered to fill the half wave zone in the FZP. The radius R_m of the m th half-wave zone is described by

$$R_m = \sqrt{m\lambda f} \quad (6)$$

where λ and f are the wavelength and the focal length, respectively. When m is an integer, a constructive interference appears at the focus. By tuning the RI of the liquid, it demonstrated the real-time modulation of the optical properties, such as peak intensity, spot size and focal length. In addition, this diffractive device is wavelength sensitive, which can selectively focus the desired wavelength. It also enables the switching between focusing, defocusing and collimation by the flow-rate control.

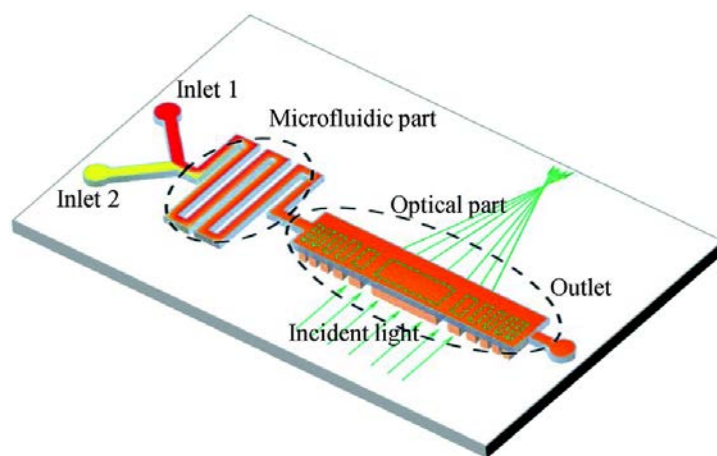


Figure 11. Schematic of the optofluidic Fresnel zone plate (FZP) [32]: it consists of a microfluidic part and an optical part. The former is used to prepare the mixed solution and the latter acts as the tunable FZP.

3. Applications of In-Plane Liquid Lenses

The in-plane optofluidic lenses can be used not only for beam manipulation, but also for some other applications in microfluidic networks, such as particle trapping. Optical tweezers utilize the tightly focused beam to trap particles in the microscale size, providing a nondestructive way to manipulate microparticles. The beam is usually focused by an objective lens with large NA and short focal length. In the traditional optical tweezer, the optical alignment is complicated, making it difficult to integrate it into a miniature lab-on-a-chip system. The emergence of optofluidics makes it easy to manipulate the particle using optical tweezers. In addition, sorting and precise moving of particle in 2D area can be easily achieved in optofluidic networks, which are difficult in conventional optical tweezers.

Yang's group proposed a reconfigurable optofluidic thermal GRIN lens and used it for single cell manipulation in the optofluidic chip [30]. As shown Figure 12, the system consists of two parts: the GRIN lens part and the cell trapping chamber. In the GRIN lens section, benzyl alcohol streams at different temperatures are pumped into the chamber to form a GRIN lens to focus the probe beam. And the living cell is contained in the cell trapping part. The cell is trapped and moved by the focused beam. By regulating the thermal lens, the trapping of the living cell can be modulated at a range of 280 μm . Recently, Aiqun Liu's group has demonstrated the manipulation of particles with sizes of several 10s nanometers using optical potential wells created by an in-plane focused beam and fluidic constraints in optofluidic chips [47,48]. The combination of the quasi-Bessel optical profile

and the loosely overdamped potential wells enable the precise manipulation of nanoparticles in the optofluidic channel. They revealed an unprecedentedly meaningful damping scenario that enriches our fundamental understanding of particle kinetics in intriguing optical systems and offered new opportunities for tumor targeting, intracellular imaging, and sorting small particles such as viruses and DNA [48]. The development in particle manipulation using the in-plane beams predicts perspective of the in-plane liquid lens.

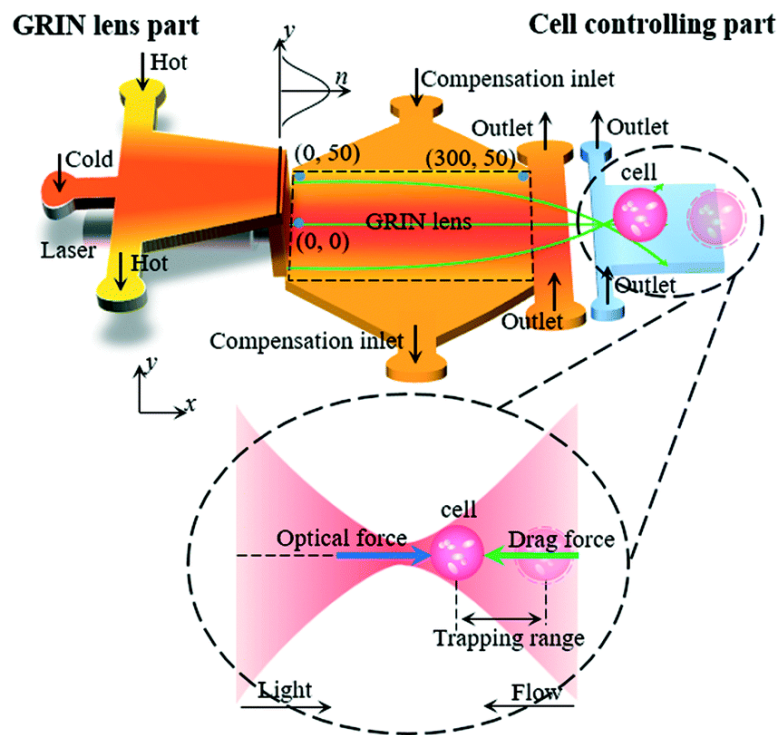


Figure 12. The schematic design of fluidic thermal GRIN lens for cell manipulation [30]: The system includes a lens chamber and a cell trapping chamber. Five streams at different temperatures are injected into the microfluidic chip to form a gradient refractive index across the channel.

The in-plane liquid lens has also been used for particle detection. Flow cytometers have been widely used for particle analysis, sorting and counting. A conventional flow cytometer consists of four main parts, including flow control, light guiding, signal collection and subsequent processing. By the use of optofluidic techniques, the flow cytometer can be integrated into a microfluidic system, reducing the size of the system and making it more portable and durable. The integration allows the benefits of including new optical features on the devices, such as built-in optical alignment, beam shaping, high optical sensitivity and high accuracy [49]. Zhang et al. gave a comprehensive review about the development of optofluidics based flow cytometers [49]. As the detected particles (or cells) are focused to a narrow stream to ensure that they pass through the optical interrogation point one by one, the measured coefficient of variation (CV) of fluorescent beads is strongly dependent on the beam geometry and bead size. As the beam coming out of the waveguide becomes divergent while it strikes at the interrogation region, a 2D lens is used to reshape and focus the beam, enhancing the beam quality for interrogation. In the past, a micro solid lens was fabricated in between the waveguide and the microchannel to improve the performance of the flow cytometer [50]. The precise fabrication of the waveguide and the solid lens system is required to ensure a good focused spot. While a reconfigurable in-plane lens allows the flexible modulation of the beam after fabrication. In addition, the tuning of the spot size makes it possible to get a low CV while detecting particles with different sizes. Goldin et al. proposed an in-plane liquid-filled lens for flow cytometer [51]. Figure 13 shows an optofluidic flow

cytometer by Nguyen's group [52]. It utilized a liquid core/liquid cladding lens to focus the light into a microchannel, where the detected particles flow through. A detection fiber was placed at the opposite side of the sample channel to collect the optical signal for subsequent processing. This compact device incorporated the optical elements and flow control part into a single chip to form a flow cytometer, instead of using bulky optics. This optofluidic flow cytometer demonstrated high efficiency and accuracy on particle counting and sizing. The detection of particles with sizes of 5, 10 and 20 μm was demonstrated. A better focused beam can significantly enhance the performance of the flow cytometers. Recently, Yang et al. gave a detail review on the development of the micro-optics for microfluidic analytical applications [53].

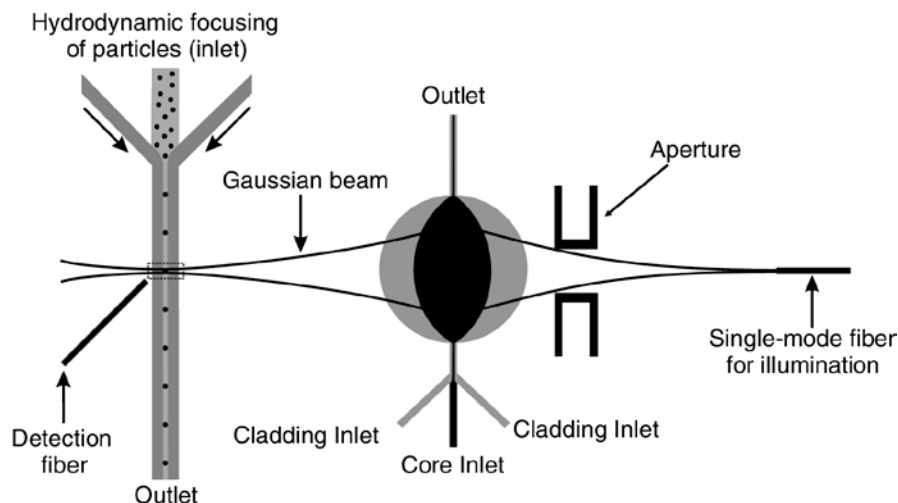


Figure 13. Schematic design of a flow cytometer using optofluidic lens [52].

4. Discussion

Different types of in-plane optofluidic lenses have been demonstrated, providing numerous methods to manipulate the light in a microfluidic network. In the previous refractive lenses, the liquid-liquid (liquid-air) interfaces are spherical, which may lead to longitudinal spherical aberration (the marginal rays are focused closer to the lens than the paraxial rays). Therefore, the beam can not be well focused into the size close to the diffraction limit. The large focused spot size limits the practical applications. For instance, the CVs in the liquid-lens-based (beam waist 23 μm) cytometer [52] are not as good as those conventional cytometers. However, the aberration can be well-suppressed in the fluidic GRIN lenses [29,30,44]. For example, the well-designed thermal lens (the spot size 4 μm) has been used to manipulate the living cells in a microfluidic network [30]. As the reflective liquid lens is modulated through pressure control or hydrodynamics, it promises better robustness. While the liquid GRIN lenses usually use the solution diffusion or the temperature gradient, which are susceptible to the ambient fluctuation. In terms of response time, the interfacial deformation takes a few seconds to switch to a new balance state. In comparison, a thermal-induced liquid lens has a faster modulated speed (it is 200 ms in [29]). Another limitation is that most of previous in-plane liquid lenses require continuous supply of liquids, which consumes a lot of liquid and reduces the compatibility of the devices. Although there are still some drawbacks, the in-plane optofluidic lenses find useful applications in lab-on-a-chip systems. In addition, the LC-based and FZP-based liquid lenses enable the polarization and wavelength manipulation in a microfluidic chip. It is foreseeable that more liquid lenses will be incorporated into a chip to achieve versatile microsystems.

5. Conclusions

This article presents a general review of in-plane optofluidic lenses. Based on their working principles and operation methods, they are categorized into three types: refractive lens, gradient index lens and others. The first two cover most of the reported designs, and the last represents some new types, such as birefringent optofluidic lenses and Fresnel zone plate liquid lenses. The in-plane optofluidic lenses have wide tunability, provide a flexible way to manipulate the beam in microfluidic networks and can be easily integrated with lab-on-a-chip systems, making them suitable for transportation and detection of the particle at the same time. It is foreseeable that the in-plane liquid lenses will make the optofluidic networks a versatile platform for research and practical applications. For instance, combining the in-plane beam shaping and microfluidic techniques enables the manipulation and analysis of the particle or cells down to nanometer scale, which may broaden our fundamental understanding of particle kinetics and be useful for biological research. A tightly focused in-plane beam can be used for sample (particle/cell) trapping, transportation, separation and detection, making it possible to construct a portable integrated system for biochemical applications.

Acknowledgments: This work is supported by National Natural Science Foundation of China (61377068), Research Grants Council of Hong Kong (N_PolyU505/13, 152184/15E and 152127/17E), and Hong Kong Polytechnic University (G-YBPR, 4-BCAL, 1-ZE14, 1-ZE27 and 1-ZVGH). Acknowledgments should also go to Materials Research Centre, University Research Facility in Material Characterization and Device Fabrication, and University Research Facility in Life Sciences of the Hong Kong Polytechnic University for the technical assistance and facility support.

Author Contributions: Qingming Chen drafted the manuscript, Tenghao Li prepared graphs, Zhaohui Li advised on the technical issues, Jinlin Long helped with the application issues and Xuming Zhang provided the idea and revised the manuscript.

Conflicts of Interest: The authors declare no conflict of interest.

References

1. Psaltis, D.; Quake, S.R.; Yang, C.H. Developing optofluidic technology through the fusion of microfluidics and optics. *Nature* **2006**, *442*, 381–386. [[CrossRef](#)] [[PubMed](#)]
2. Zhao, Y.; Stratton, Z.S.; Guo, F.; Lapsley, M.I.; Chan, C.Y.; Lin, S.-C.S.; Huang, T.J. Optofluidic imaging: Now and beyond. *Lab Chip* **2013**, *13*, 17–24. [[CrossRef](#)] [[PubMed](#)]
3. Monat, C.; Domachuk, P.; Eggleton, B.J. Integrated optofluidics: A new river of light. *Nat. Photon.* **2007**, *1*, 106–114. [[CrossRef](#)]
4. Fan, X.D.; White, I.M. Optofluidic Microsystems for Chemical and Biological Analysis. *Nat. Photon.* **2011**, *5*, 591–597. [[CrossRef](#)] [[PubMed](#)]
5. Pang, L.; Chen, H.M.; Freeman, L.M.; Fainman, Y. Optofluidic devices and applications in photonics, sensing and imaging. *Lab Chip* **2012**, *12*, 3543–3551. [[CrossRef](#)] [[PubMed](#)]
6. Chen, Y.F.; Jiang, L.; Mancuso, M.; Jain, A.; Oncescu, V.; Erickson, D. Optofluidic opportunities in global health, food, water and energy. *Nanoscale* **2012**, *4*, 4839–4857. [[CrossRef](#)] [[PubMed](#)]
7. Erickson, D.; Sinton, D.; Psaltis, D. Optofluidics for energy applications. *Nat. Photon.* **2011**, *5*, 583–590. [[CrossRef](#)]
8. Levy, U.; Shamai, R. Tunable optofluidic devices. *Microfluid. Nanofluidics* **2007**, *4*, 97–105. [[CrossRef](#)]
9. Monat, C.; Domachuk, P.; Grillet, C.; Collins, M.; Eggleton, B.J.; Cronin-Golomb, M.; Mutzenich, S.; Mahmud, T.; Rosengarten, G.; Mitchell, A. Optofluidics: A novel generation of reconfigurable and adaptive compact architectures. *Microfluid. Nanofluidics* **2007**, *4*, 81–95. [[CrossRef](#)]
10. Erickson, D. Optofluidics. In *Microfluidics Based Microsystems*; Springer: Dordrecht, The Netherlands, 2010; pp. 529–551.
11. Hunt, H.C.; Wilkinson, J.S. Optofluidic integration for microanalysis. *Microfluid. Nanofluidics* **2008**, *4*, 53–79. [[CrossRef](#)]
12. Nguyen, N.-T. Micro-optofluidic Lenses: A review. *Biomicrofluidics* **2010**, *4*, 031501. [[CrossRef](#)] [[PubMed](#)]
13. Fan, X.D.; Yun, S.H. The potential of optofluidic biolasers. *Nat. Methods* **2014**, *11*, 141–147. [[CrossRef](#)] [[PubMed](#)]

14. Mandal, S.; Erickson, D. Nanoscale optofluidic sensor arrays. *Opt. Express* **2008**, *16*, 1623–1631. [[CrossRef](#)] [[PubMed](#)]
15. Kühn, S.; Measor, P.; Lunt, E.J.; Phillips, B.S.; Deamer, D.W.; Hawkins, A.R.; Schmidt, H. Loss-based optical trap for on-chip particle analysis. *Lab Chip* **2009**, *9*, 2212–2216. [[CrossRef](#)] [[PubMed](#)]
16. Schmidt, B.S.; Yang, A.H.; Erickson, D.; Lipson, M. Optofluidic trapping and transport on solid core waveguides within a microfluidic device. *Opt. Express* **2007**, *15*, 14322–14334. [[CrossRef](#)] [[PubMed](#)]
17. Shopova, S.I.; Zhou, H.Y.; Fan, X.D.; Zhang, P. Optofluidic ring resonator based dye laser. *Appl. Phys. Lett.* **2007**, *90*, 221101. [[CrossRef](#)]
18. Tang, S.K.Y.; Mayers, B.T.; Vezenov, D.V.; Whitesides, G.M. Optical waveguiding using thermal gradients across homogeneous liquids in microfluidic channels. *Appl. Phys. Lett.* **2006**, *88*, 061112. [[CrossRef](#)]
19. Yang, Y.; Liu, A.Q.; Chin, L.K.; Zhang, X.M.; Tsai, D.P.; Lin, C.L.; Lu, C.; Wang, G.P.; Zheludev, N.I. Optofluidic waveguide as a transformation optics device for lightwave bending and manipulation. *Nat. Commun.* **2012**, *3*, 651. [[CrossRef](#)] [[PubMed](#)]
20. Kuiper, S.; Hendriks, B.H.W. Variable-focus liquid lens for miniature cameras. *Appl. Phys. Lett.* **2004**, *85*, 1128–1130. [[CrossRef](#)]
21. Chiu, C.P.; Chiang, T.J.; Chen, J.K.; Chang, F.C.; Ko, F.-H.; Chu, C.W.; Kuo, S.-W.; Fan, S.K. Liquid Lenses and Driving Mechanisms: A Review. *J. Adhes. Sci. Technol.* **2012**, *26*, 1773–1788. [[CrossRef](#)]
22. Mishra, K.; van den Ende, D.; Mugele, F. Recent Developments in Optofluidic Lens Technology. *Micromachines* **2016**, *7*, 102. [[CrossRef](#)]
23. Xu, S.; Ren, H.W.; Wu, S.T. Dielectrophoretically tunable optofluidic devices. *J. Phys. D Appl. Phys.* **2013**, *46*, 483001. [[CrossRef](#)]
24. Krogmann, F.; Monch, W.; Zappe, H. Electrowetting for Tunable Microoptics. *J. Microelectromech. Syst.* **2008**, *17*, 1501–1512. [[CrossRef](#)]
25. Shi, J.; Stratton, Z.; Lin, S.C.S.; Huang, H.; Huang, T.J. Tunable optofluidic microlens through active pressure control of an air–liquid interface. *Microfluid. Nanofluidics* **2009**, *9*, 313–318. [[CrossRef](#)]
26. Mao, X.L.; Waldeisen, J.R.; Juluri, B.K.; Huang, T.J. Hydrodynamically tunable optofluidic cylindrical microlens. *Lab Chip* **2007**, *7*, 1303–1308. [[CrossRef](#)] [[PubMed](#)]
27. Fang, C.L.; Dai, B.; Xu, Q.; Zhuo, R.; Wang, Q.; Wang, X.; Zhang, D.W. Hydrodynamically reconfigurable optofluidic microlens with continuous shape tuning from biconvex to biconcave. *Opt. Express* **2017**, *25*, 888–897. [[CrossRef](#)] [[PubMed](#)]
28. Mao, X.L.; Lin, S.C.S.; Lapsley, M.I.; Shi, J.; Juluri, B.K.; Huang, T.J. Tunable Liquid Gradient Refractive Index (L-GRIN) lens with two degrees of freedom. *Lab Chip* **2009**, *9*, 2050–2058. [[CrossRef](#)] [[PubMed](#)]
29. Chen, Q.M.; Jian, A.Q.; Li, Z.H.; Zhang, X.M. Optofluidic tunable lenses using laser-induced thermal gradient. *Lab Chip* **2016**, *16*, 104–111. [[CrossRef](#)] [[PubMed](#)]
30. Liu, H.L.; Shi, Y.; Liang, L.; Li, L.; Guo, S.S.; Yin, L.; Yang, Y. A liquid thermal gradient refractive index lens and using it to trap single living cell in flowing environments. *Lab Chip* **2017**, *17*, 1280–1286. [[CrossRef](#)] [[PubMed](#)]
31. Wee, D.; Hwang, S.H.; Song, Y.S.; Youn, J.R. Tunable optofluidic birefringent lens. *Soft Matter* **2016**, *12*, 3868–3876. [[CrossRef](#)] [[PubMed](#)]
32. Shi, Y.; Zhu, X.Q.; Liang, L.; Yang, Y. Tunable focusing properties using optofluidic Fresnel zone plates. *Lab Chip* **2016**, *16*, 4554–4559. [[CrossRef](#)] [[PubMed](#)]
33. Tang, S.K.; Stan, C.A.; Whitesides, G.M. Dynamically reconfigurable liquid-core liquid-cladding lens in a microfluidic channel. *Lab Chip* **2008**, *8*, 395–401. [[CrossRef](#)] [[PubMed](#)]
34. Liang, D.; Jiang, H.R. Selective Formation and Removal of Liquid Microlenses at Predetermined Locations Within Microfluidics through Pneumatic Control. *J. Microelectromech. Syst.* **2008**, *17*, 381–392. [[CrossRef](#)]
35. Hsiung, S.K.; Lee, C.H.; Lee, G.B. Microcapillary electrophoresis chips utilizing controllable micro-lens structures and buried optical fibers for on-line optical detection. *Electrophoresis* **2008**, *29*, 1866–1873. [[CrossRef](#)] [[PubMed](#)]
36. Seow, Y.C.; Liu, A.Q.; Chin, L.K.; Li, X.C.; Huang, H.J.; Cheng, T.H.; Zhou, X.Q. Different curvatures of tunable liquid microlens via the control of laminar flow rate. *Appl. Phys. Lett.* **2008**, *93*, 084101. [[CrossRef](#)]
37. Song, C.; Nguyen, N.T.; Tan, S.H.; Asundi, A.K. Modelling and optimization of micro optofluidic lenses. *Lab Chip* **2009**, *9*, 1178–1184. [[CrossRef](#)] [[PubMed](#)]

38. Li, H.; Song, C.; Luong, T.D.; Nguyen, N.T.; Wong, T.N. An electrokinetically tunable optofluidic bi-concave lens. *Lab Chip* **2012**, *12*, 3680–3687. [[CrossRef](#)] [[PubMed](#)]
39. Chao, K.S.; Lin, M.S.; Yang, R.J. An in-plane optofluidic microchip for focal point control. *Lab Chip* **2013**, *13*, 3886–3892. [[CrossRef](#)] [[PubMed](#)]
40. Seow, Y.C.; Lim, S.P.; Lee, H.P. Optofluidic variable-focus lenses for light manipulation. *Lab Chip* **2012**, *12*, 3810–3815. [[CrossRef](#)] [[PubMed](#)]
41. Yang, Y.; Chin, L.K.; Tsai, J.M.; Tsai, D.P.; Zheludev, N.I.; Liu, A.Q. Transformation optofluidics for large-angle light bending and tuning. *Lab Chip* **2012**, *12*, 3785–3790. [[CrossRef](#)] [[PubMed](#)]
42. Liu, H.L.; Zhu, X.Q.; Liang, L.; Zhang, X.M.; Yang, Y. Tunable transformation optical waveguide bends in liquid. *Optica* **2017**, *4*, 839–846. [[CrossRef](#)]
43. Shi, Y.; Liang, L.; Zhu, X.Q.; Zhang, X.M.; Yang, Y. Tunable self-imaging effect using hybrid optofluidic waveguides. *Lab Chip* **2015**, *15*, 4398–4403. [[CrossRef](#)] [[PubMed](#)]
44. Zhao, H.T.; Yang, Y.; Chin, L.K.; Chen, H.F.; Zhu, W.M.; Zhang, J.B.; Yap, P.H.; Liedberg, B.; Wang, K.; Wang, G.; et al. Optofluidic lens with low spherical and low field curvature aberrations. *Lab Chip* **2016**, *16*, 1617–1624. [[CrossRef](#)] [[PubMed](#)]
45. Wolfe, D.B.; Vezenov, D.V.; Mayers, B.T.; Whitesides, G.M.; Conroy, R.S.; Prentiss, M.G. Diffusion-controlled optical elements for optofluidics. *Appl. Phys. Lett.* **2005**, *87*, 181105. [[CrossRef](#)]
46. Lin, H.C.; Chen, M.S.; Lin, Y.H. A Review of Electrically Tunable Focusing Liquid Crystal Lenses. *Trans. Electr. Electron. Mater.* **2011**, *12*, 234–240. [[CrossRef](#)]
47. Shi, Y.Z.; Xiong, S.; Chin, L.K.; Yang, Y.; Zhang, J.B.; Ser, W.; Wu, J.H.; Chen, T.N.; Yang, Z.C.; Hao, Y.L.; et al. High-resolution and multi-range particle separation by microscopic vibration in an optofluidic chip. *Lab Chip* **2017**, *17*, 2443–2450. [[CrossRef](#)] [[PubMed](#)]
48. Shi, Y.Z.; Xiong, S.; Chin, L.K.; Zhang, J.B.; Ser, W.; Wu, J.H.; Chen, T.N.; Yang, Z.C.; Hao, Y.L.; Liedberg, B.; et al. Nanometer-precision linear sorting with synchronized optofluidic dual barriers. *Sci. Adv.* **2018**, *4*, eaao0773. [[CrossRef](#)] [[PubMed](#)]
49. Zhang, Y.S.; Watts, B.R.; Guo, T.Y.; Zhang, Z.Y.; Xu, C.Q.; Fang, Q.Y. Optofluidic Device Based Microflow Cytometers for Particle/Cell Detection: A Review. *Micromachines* **2016**, *7*, 70. [[CrossRef](#)]
50. Watts, B.R.; Zhang, Z.Y.; Xu, C.Q.; Cao, X.D.; Lin, M. Scattering detection using a photonic-microfluidic integrated device with on-chip collection capabilities. *Electrophoresis* **2014**, *35*, 271–281. [[CrossRef](#)] [[PubMed](#)]
51. Godin, J.; Lien, V.; Lo, Y.H. Demonstration of two-dimensional fluidic lens for integration into microfluidic flow cytometers. *Appl. Phys. Lett.* **2006**, *89*, 061106. [[CrossRef](#)]
52. Song, C.; Luong, T.D.; Kong, T.F.; Nguyen, N.T.; Asundi, A.K. Disposable flow cytometer with high efficiency in particle counting and sizing using an optofluidic lens. *Opt. Lett.* **2011**, *36*, 657–659. [[CrossRef](#)] [[PubMed](#)]
53. Yang, H.; Gijs, M.A.M. Micro-optics for microfluidic analytical applications. *Chem. Soc. Rev.* **2018**, in press. [[CrossRef](#)] [[PubMed](#)]

